The Astrophysical Journal, 792:115 (6pp), 2014 September 10 doi:10.1088/0004-637X/792/2/115

HUBBLE SPACE TELESCOPE OBSERVATIONS OF THE AFTERGLOW, SUPERNOVA, AND HOST GALAXY ASSOCIATED WITH THE EXTREMELY BRIGHT GRB 130427A

A. J. Levan[1], N. R. Tanvir[2], A. S. Fruchter[3], J. Hjorth[4], E. Pian[5,6,7], P. Mazzali[8], R. A. Hounsell[3], D. A. Perley[9,15], Z. Cano[10], J. Graham[3], S. B. Cenko[11], J. P. U. Fynbo[4], C. Kouveliotou[12], A. Pe'er[13], K. Misra[14], and K. Wiersema[2]
[1] Department of Physics, University of Warwick, Coventry, CV4 7AL, UK; a.j.levan@warwick.ac.uk
[2] Department of Physics and Astronomy, University of Leicester, University Road, Leicester, LE1 7RH, UK
[3] Space Telescope Science Institute, 3700 San Martin Drive, Baltimore, MD 21218, USA
[4] Dark Cosmology Centre, Niels Bohr Institute, University of Copenhagen, Juliane Maries Vej 30, DK-2100 Copenhagen, Denmark
[5] INAF, Trieste Astronomical Observatory, via G.B. Tiepolo 11, I-34143 Trieste, Italy
[6] Scuola Normale Superiore, Piazza dei Cavalieri 7, I-56126 Pisa, Italy
[7] European Southern Observatory, Karl-Schwarzschild-Strasse 2, D-85748 Garching bei München, Germany
[8] Astrophysics Research Institute, Liverpool John Moores University, IC2 Liverpool Science Park 146 Brownlow Hill, Liverpool L3 5RF, UK
[9] Department of Astronomy, California Institute of Technology, MC 249-17, 1200 East California Blvd., Pasadena, CA 91125, USA
[10] Centre for Astrophysics and Cosmology, Science Institute, University of Iceland, Dunhagi 5, 107 Reykjavik, Iceland
[11] Astrophysics Science Division, NASA Goddard Space Flight Center, Mail Code 661, Greenbelt, MD 20771, USA
[12] Science and Technology Office, ZP12, NASA/Marshall Space Flight Center, Huntsville, AL 35812, USA
[13] Department of Physics, University College Cork, Cork, Ireland
[14] Aryabhatta Research Institute of Observational Sciences, Manora Peak, Nainital-263 002, India
Received 2013 July 19; accepted 2014 June 18; published 2014 August 22

ABSTRACT

We present *Hubble Space Telescope* (*HST*) observations of the exceptionally bright and luminous *Swift* gamma-ray burst (GRB), GRB 130427A. At $z = 0.34$, this burst affords an excellent opportunity to study the supernova (SN) and host galaxy associated with an intrinsically extremely luminous burst ($E_{\rm iso} > 10^{54}$ erg): more luminous than any previous GRB with a spectroscopically associated SN. We use the combination of the image quality, UV capability, and invariant point-spread function of *HST* to provide the best possible separation of the afterglow, host, and SN contributions to the observed light ∼17 rest-frame days after the burst, utilizing a host subtraction spectrum obtained one year later. Advanced Camera for Surveys grism observations show that the associated SN, SN 2013cq, has an overall spectral shape and luminosity similar to SN 1998bw (with a photospheric velocity, $v_{\rm ph} \sim 15{,}000$ km s^{-1}). The positions of the bluer features are better matched by the higher velocity SN 2010bh ($v_{\rm ph} \sim 30{,}000$ km s^{-1}), but this SN is significantly fainter and fails to reproduce the overall spectral shape, perhaps indicative of velocity structure in the ejecta. We find that the burst originated ∼4 kpc from the nucleus of a moderately star forming ($1\,M_{\odot}$ yr^{-1}), possibly interacting disk galaxy. The absolute magnitude, physical size, and morphology of this galaxy, as well as the location of the GRB within it, are also strikingly similar to those of GRB 980425/SN 1998bw. The similarity of the SNe and environment from both the most luminous and least luminous GRBs suggests that broadly similar progenitor stars can create GRBs across six orders of magnitude in isotropic energy.

Key words: gamma-ray burst: general – supernovae: general

Online-only material: color figures

1. INTRODUCTION

The connection between long duration gamma-ray bursts (LGRBs) and hydrogen-poor type Ic supernovae (SNe Ic) has become well-established based on the detection of spectroscopic signatures of these supernovae (SNe) accompanying a handful of relatively local GRBs (e.g., Hjorth et al. 2003; Stanek et al. 2003; Soderberg et al. 2004; Pian et al. 2006; Bufano et al. 2012). The GRB–SNe sample increases when combined with a larger set of events that exhibit photometric signatures in their light curves, consistent with SNe Ic (see, e.g., Cano 2013). Although, these light curve "humps" are not uniquely diagnostic of the SN type, and are open to alternative interpretations, the emerging scenario is that the majority of long GRBs are associated with SNe Ic (e.g., Cano 2013).

However, the picture painted by observations of such GRB–SNe pairs has remained unsatisfactory in some respects. On average, these local events differ substantially from the majority of the GRB population in terms of energy release, with isotropic energy releases ($E_{\rm iso}$) a factor of 10^2–10^4 lower than the bulk population (e.g., Kaneko et al. 2007). Of the bursts with the strongest evidence for SNe, only GRB 030329, with $E_{\rm iso} \sim 10^{52}$ erg, appears close to being a classical cosmological long-GRB. Several local GRB/SNe pairs exhibit γ-ray emission of extremely long duration (Campana et al. 2006; Starling et al. 2011), while other very long events at larger redshift show little evidence for SNe (Levan et al. 2014). Indeed, these local, low-luminosity bursts have been suggested to arise from a very different physical mechanism than the classical bursts, such as relativistic shock break-out from the SN itself (e.g., Nakar & Sari 2012). Such emission is difficult to locate in more luminous GRBs due to a combination of distance and glare from the burst itself, though evidence for possible shock break-out components has been found in some GRBs (Starling et al. 2012; Sparre & Starling 2012). However, the several order of magnitude difference in energy release between the local, low-luminosity and cosmological, high luminosity GRBs could also be indicative of rather different physical mechanisms at play. Given this, the nature of the connection between the most energetic GRBs and their SNe remains in urgent need of further study.

[15] Hubble Fellow.

Table 1
Log of *HST* Observations of GRB 130427A

Date-obs (yy-mm-dd)	MJD-obs	ΔT (days)	Filter	Exp. (s)	AB-magnitude
2013-May-20	56432.10521	22.78	F336W	1266	23.280 ± 0.02
2013-May-20	56432.12503	22.80	F160W	1048	21.604 ± 0.01
2013-May-20	56432.37207	23.05	F606W	180	21.760 ± 0.01
2013-May-20	56432.37603	23.05	G800L	1880	...
2014-Apr-12	56759.14866	349.82	F336W	2508	26.17 ± 0.09
2014-Apr-18	56765.18459	355.86	F606W	180	25.67 ± 0.11
2014-Apr-18	56765.18459	355.86	G800L	1880	...

Notes. Log of *HST* observations of GRB 130427A. Optical observations were obtained with ACS, while UV and IR imaging was taken with WFC3 in the UVIS and IR channels respectively. The magnitudes shown are for a point source at the GRB location and not for the overall host galaxy + afterglow combination. The magnitudes are corrected for a foreground extinction of $A_{F336W} = 0.090$ mag, $A_{F606W} = 0.050$ mag, and $A_{F160W} = 0.010$ mag. Errors in the magnitudes are only statistical.

Here, we report observations of the brightest (highest fluence) GRB detected in the past ~20 yr, GRB 130427A. The isotropic energy release of $E_{\rm iso} \sim 10^{54}$ erg, places it in the most luminous 5% of GRBs observed to date by *Swift*, and a factor of 100 brighter than GRB 030329 (Hjorth et al. 2003), which was the most luminous GRB with a well-studied SN. At a redshift of $z = 0.340$ (Levan et al. 2013; Xu et al. 2013; Perley et al. 2014), the burst is close enough that any SN is open to spectroscopic study, and indeed the presence of an SN, SN 2013cq, has been established (de Ugarte Postigo et al. 2013; Xu et al. 2013). Here, we use the resolution of the *Hubble Space Telescope* (*HST*) to resolve and dramatically reduce the galaxy contribution and its UV capability to track the afterglow, hence enabling a view of the SN as free as possible from the host, afterglow, and atmospheric hinderance.

2. OBSERVATIONS

GRB 130427A was discovered by *Swift* at 07:47:57 UT on 2013 April 27 (Maselli et al. 2013). It was also detected as an exceptionally bright GRB by *Konus-WIND* and *Fermi* with the Gamma-ray Burst Monitor (GBM; von Kienlin 2013) and LAT (Zhu et al. 2013), and its prompt fluence of $S \approx 3 \times 10^{-3}$ erg cm^{-2} in the 10–1000 keV band (von Kienlin 2013) makes it the most fluent GRB observed by *Swift*, *Fermi*, or BATSE. It showed a bright X-ray and optical afterglow, peaking at $R = 7.4$ before the *Swift* GRB trigger (Wren et al. 2013). Early spectroscopy of the afterglow yielded a redshift of $z = 0.340$ (Levan et al. 2013), which was confirmed from later, more detailed, spectroscopic observations (Xu et al. 2013). A full description of the afterglow is given in Perley et al. (2014) and Maselli et al. (2014). Deep photometric and spectroscopic observations over the first 10 days post burst revealed a rebrightening, consistent with the presence of an SNe Ic, SN 2013cq (de Ugarte Postigo et al. 2013; Xu et al. 2013).

2.1. Hubble Space Telescope Observations

We observed the location of GRB 130427A with *HST* on 2013 May 20, 23 days after the initial burst detection. A second epoch was obtained in 2014 April, almost a year after the initial burst. A log of these observations is shown in Table 1. For a more detailed study of the host galaxy we also utilize a longer (2228 s) WFC3/F606W observation obtained on 2014 May 15. The imaging data were reduced in the standard fashion; with on-the-fly processed data retrieved from the archive and subsequently redrizzled using `astrodrizzle`, for UVIS observations we separately corrected for pixel-based charge-transfer inefficiency (CTE; Anderson & ACS Team 2012; Anderson 2014). Photometry was performed in small apertures to minimize any contribution from underlying galaxy light, and maximize signal-to-noise, it was subsequently corrected using standard aperture corrections.[16] We also use direct image subtraction to isolate the afterglow/SNe light at early epochs, this effectively removes the host contribution. These magnitudes may still contain some transient light, but since the second epoch magnitudes are a factor of ~15–30 lower than observed at early times, this suggests that these epochs can be used for effective subtraction.The resulting photometry is shown in Table 1, while our *HST* images are shown in Figure 1.

We also obtained grism spectroscopy centered at ~8000 Å with the G800L grism on the Advanced Camera for Surveys (ACS), with a position angle chosen to minimize the contribution from the underlying host galaxy (see Figure 1). Again, we utilized the on-the-fly calibrated images, corrected for CTE and bias striping. We detected sources on a single F606W image and extracted these via `aXe`, subsequently drizzling each of the four exposures to create master spectra, which was flux calibrated using published sensitivity curves. We extracted the light from the GRB counterpart in a relatively small aperture (~2 × FWHM). In principle, a given pixel in the grism image may be exposed to light of multiple different wavelengths from different spatial locations on the chip. For the second epoch of observations, we force an extraction of the same width at the position of the transient (as determined by a map between the first and second epoch of direct imaging). We then subtract this from the initial spectrum to obtain a host free spectrum. Since we have utilized a tight aperture around the SNe, we subsequently scale this subtracted spectrum to the host subtracted magnitudes of the afterglow/SNe.

3. ISOLATING THE SUPERNOVA

3.1. Host Contamination

The afterglow is offset $(0.83 \pm 0.03)''$ from the centroid of the host galaxy light in F606W, and thus the latter is of little concern in our small ($0\farcs1$) apertures. However, regions underlying GRBs are frequently among the most luminous parts of their hosts (Fruchter et al. 2006); therefore, some contamination may be expected. Our late time subtraction removes this from both our broadband photometry and grism spectroscopy. For the high-resolution observations reported here, this contamination is small (at most 6% in the UV and 3% in the optical) for our photometry. However, the contribution is somewhat larger in the grism observations. These observations disperse light not only from the region directly underlying the GRB, but also from other locations in the host (which represent contributions at different wavelengths, overlapping the transient light). In particular, the proximate, bright star-forming region considerably contaminates the SNe (>20% at the red end of our spectrum beyond 9000 Å). This region is also likely to be the dominant host contaminant in ground-based spectroscopy (since the host galaxy is resolved), and has quite different colors from the global host, implying potentially significant systematic errors when the broadband Sloan Digital Sky Survey (SDSS) colors of the host are used to attempt a subtraction (e.g., Xu et al. 2013; Melandri et al. 2014). Here, we can directly remove this contribution via the subtraction of the deep second epoch.

[16] See Sirianni et al. (2005) for ACS aperture corrections and http://www.stsci.edu/hst/wfc3/phot_zp_lbn for WFC3.

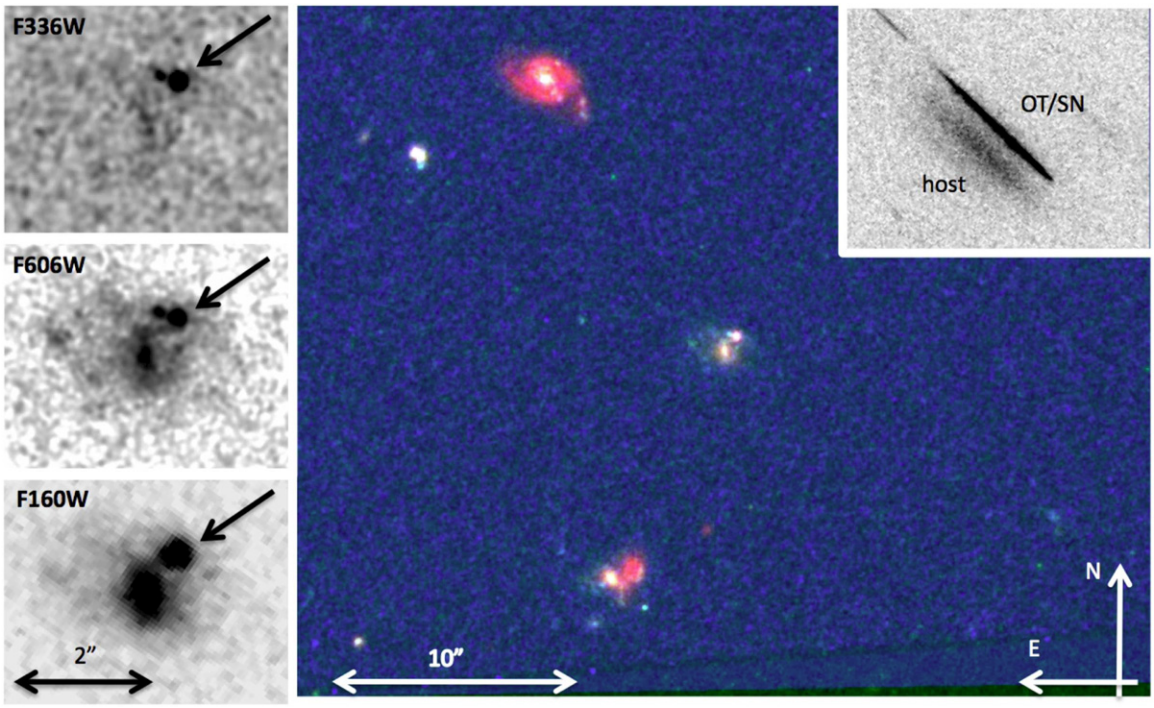

Figure 1. *HST* observations of GRB 130427A. The left panel shows our UV–optical and IR imaging (the UV data taken on 2013 May 20 and the optical/IR on 2013 July 10). The afterglow, indicated by an arrow, can be clearly seen offset 0.″83 from the center of its host galaxy. In the UV, the host is weakly detected, with a strong star-forming region seen to the east of the GRB location. The F606W image shows a disk galaxy with hints of a bar structure, along with some signs of distortion possibly due to ongoing interaction. The large central panel shows a color image from the three-band *HST* imaging. The host is at the center, while other galaxies, possibly part of a structure at the same redshift, are visible. The top right panel shows our grism spectroscopy of the host galaxy with the counterpart dispersed away from the host galaxy.

(A color version of this figure is available in the online journal.)

3.2. Afterglow

SNe Ib/c are generally weak UV emitters due to the strong metal line blanketing shortward of ∼3000 Å; therefore, to first order our F336W observations should be free of SN contribution. This is consistent with the UV colors of GRB 060218/SN 2006aj (from Šimon et al. 2010) and of XRF100316D/SN 2010bh (from Cano et al. 2011), which would predict a factor >10 decrease in flux between F606W and F336W. There are few UV spectra of SN Ic; however, if we graft the STIS UV observations of SN 2002ap onto the optical spectra of SN 1998bw following Levan et al. 2005, then we can obtain a first-order approximation of the likely UV spectral shape (see Figure 2).

These colors and spectra suggest that it is reasonable to assume that the F336W light is dominated by the afterglow component. To confirm this, we utilize the UV to IR light curve from Perley et al. (2014). This exhibits a spectral slope of $F_\nu \propto \nu^\beta$ with $\beta \approx -0.92$ and predicts $U(\mathrm{AB}) = 23.41 \pm 0.10$ at the time of the first epoch of *HST* F336W observations. The corresponding *HST* UV magnitude is F336W(AB) = 23.28 ± 0.02. Corrected for foreground absorption, this is consistent with the afterglow contributing 90% ± 10% of the measured F336W flux, confirming our assumptions above. This afterglow model predicts F160W(AB) = 21.84, somewhat fainter than the measured magnitude and suggesting that the SN makes up ∼20% of the light in this band, again in keeping with expectations of the few IR spectra of broad-lined SNe Ic obtained to-date (e.g., Bufano et al. 2012).

We estimate the SN contribution by using the model above, with initial error bars accounting for the uncertainty in the F336W afterglow light discussed above and the intrinsic value of β, which we adopt to be 0.92 ± 0.1. For this range of models, we then subtract the afterglow spectrum from the measured grism data and neglect any host galaxy contamination. The extremum of this model is set by the assumption that both F336W and F160W are entirely dominated by afterglow, and by subtracting the resulting power-law index.

4. DISCUSSION

4.1. Supernova Properties

Our grism spectrum, both before and after subtraction of the afterglow and host light, is shown in Figure 2 (top and bottom). Broad features, consistent with those seen in other high velocity SN Ic associated with GRBs are clearly visible in the spectrum, even before the subtraction of the afterglow component. The absence of broad emission at Hα or He absorption rules out type II or Ib events, respectively. In the lower panel of Figure 2, we plot rest-frame wavelength versus luminosity comparisons of the afterglow subtracted and dereddened[17] spectra of SN 2013cq with various GRB/SNe pairs.

The closest match for the overall spectral shape and luminosity is that of SN 1998bw (Galama et al. 1998; Iwamoto et al. 1998; Patat et al. 2001). The similarity in appearance of these SNe is primarily due to the overall spectral shape, with a drop in luminosity of a factor of ∼3 over the 5000–7000 Å range, substantially more than seen in other GRB/SNe pairs.

[17] We deredden the spectra with a Fitzpatrick (1999) law, for a Galactic $E(B-V) = 0.02$ and intrinsic $E(B-V) = 0.05$, consistent with the Na I D Doublet (Xu et al. 2013) and afterglow modeling (Perley et al. 2014; Maselli et al. 2014). The comparison SNe have been dereddened, utilizing $E(B-V) = 0.07$ for SN 1998bw and a range of $E(B-V)$ for SN 2010bh. The spectrum of SN 2003dh is from a spectral model free from extinction.

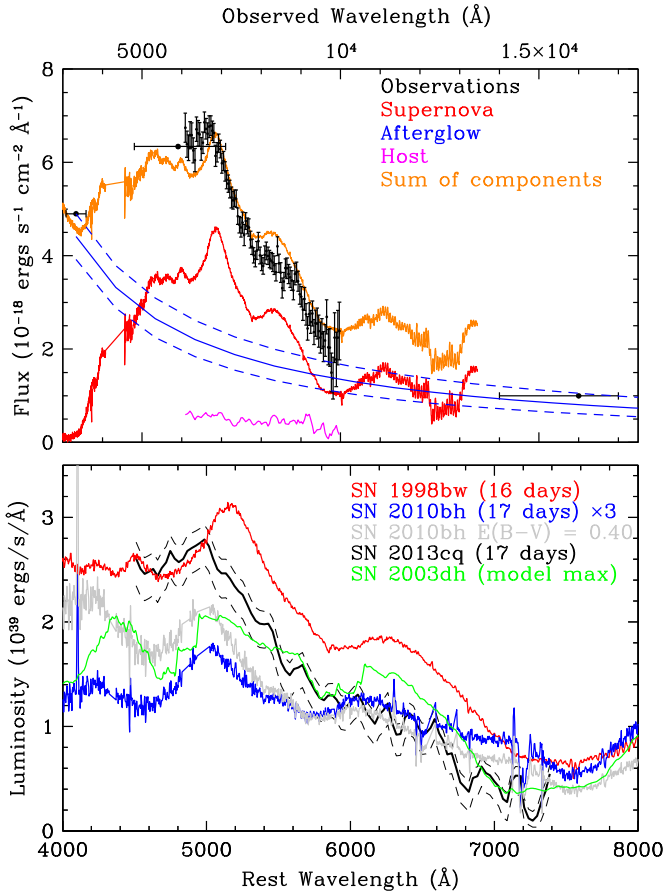

Figure 2. Spectral energy distribution of GRB 130427A/SN 2013cq as measured with *HST*. The top panel shows the data (black) along with the different components that may contribute as indicated. The host galaxy spectrum is based on our extraction of the host directly under the GRB position, and not its global properties. The lower panel shows the smoothed SN spectrum after subtraction of the afterglow light, and in luminosity space, directly compared with spectra of other GRB/SNe pairs. The supernovae have been scaled as shown in the legend, but in general the spectra show a good match with SN 1998bw at a similar epoch.

(A color version of this figure is available in the online journal.)

The broad colors of these SNe are similar, and if the kink at ∼6000 Å is interpreted as the Si II (6355 Å) blend, then it would be indicative of a photospheric velocity similar to SN 1998bw at the same epoch ($v_{\rm ph} \sim 15{,}000$ km s^{-1}), though we note that this feature is apparently stronger in SN 1998bw, where there is marked upturn in flux redward of it. This may suggest a somewhat higher velocity for SN 2013cq. Taken at face value, this would suggest that SN 2013cq is broadly similar in peak luminosity, ^{56}Ni production and kinetic energy to SN 1998bw.

While the similarity to SN 1998bw is very marked over the rest-frame spectral range from 5100–7000 Å it is much poorer around the central peak of an SN Ic at ∼5000 Å. In SN 2013cq this feature appears to be broader and blueshifted relative to SN 1998bw, as observed by Xu et al. (2013). Our comparison suggests that this peak may fit better with the slightly higher velocity SN 2003dh (Hjorth et al. 2003; Mazzali et al. 2003), the only one of the comparison SNe to arise from a luminous cosmological GRB. In this case, the SN 2003dh model shown in Figure 2 remains a factor of 50% less luminous than SN 2013cq, and is systematically redder (i.e., a smaller decrement between the peak and ∼6000 Å). However, the positions of the broadened lines do then appear generally similar.

Alternatively, this could be suggestive of a much higher velocity SN such as SN 2010bh (Bufano et al. 2012; Cano et al. 2011) as favored by Xu et al. (2013), who infer $v_{\rm ph} = 32{,}000$ km s^{-1} from the Fe II (5169 Å) at an epoch of 12.5 rest-frame days. This does provide a good match to the location and width of the feature; however, the overall spectral shape and luminosity of SN 2010bh are also very different from SN 2013cq. At 17 days, SN 2013cq appears to be much bluer and a factor >3 times more luminous than SN 2010bh, suggesting that it is not as good of an analog as SN 1998bw. To obtain a match in both luminosity and general spectral shape would require that the reddening in the direction of SN 2010bh had been significantly underestimated. Our plotted spectrum assumes $E(B-V)_{\rm gal} = 0.12$ and $E(B-V)_{\rm int} = 0.14$ (Bufano et al. 2012). To obtain a match would require dereddening the spectra with an *additional* $E(B-V) = 0.4$–0.5, well beyond the values allowed from the Na I D doublet observed in moderate resolution X-shooter spectroscopy (Bufano et al. 2012) and even the largest extinctions allowed by the afterglow spectrum (Olivares E. et al. 2012). Hence, we disfavor the suggestion that the underlying SNe is similar to SN 2010bh, due to the significant disparity in the luminosity. Instead, we favor an SNe similar in ^{56}Ni yield and kinetic energy to SN 1998bw and SN 2003dh, in which possible velocity structure within the ejecta gives rise to a range of features within the spectra that do not provide a unique match to any previous GRB/SNe pair. Indeed, the recent study of Melandri et al. (2014) also identifies a source that is much brighter than SN 2010bh, but spectrally intermediate between SN 1998bw and SN 2010bh.

Despite these differences, it is clear that the features observed in the spectrum of SN 2013cq are broadly compatible to the range observed in SN/GRB pairs, though a full model description of the spectrum is beyond the scope of this paper. To obtain approximate bounds on the luminosity of the SN, we integrate our afterglow and host subtracted spectra (allowing for the errors in the afterglow parameters) through a rest-frame V-band filter to obtain a luminosity relative to SN 1998bw. This suggests that SN 2013cq has a luminosity factor $k = L_V(2013{\rm cq})/L_V(1998{\rm bw})$ of 0.77 ± 0.10. Given the suggestions that SN 2013cq is more rapidly evolving than SN 1998bw (Xu et al. 2013), these observations (at the V-band peak of SN 1998bw) may underestimate by true peak luminosity, which may be even closer to that of SN 1998bw.

GRB 130427A is unusual as a luminous GRB at a redshift at which the SNe are open to detailed study. Indeed, it is the highest luminosity burst for which there is spectroscopic evidence for an SN. In this regard, the similarity of the SN to that seen in a burst (GRB 980425) that was six orders of magnitude less energetic is striking. As we show in Figure 3, there is no correlation between the GRB energetics and the inferred peak magnitudes of their SNe. These similarities in SNe peak luminosity, and in their spectra, suggest similarities in the ejected ^{56}Ni masses and kinetic energies. Recent modeling (Mazzali et al. 2013) has used these diagnostics to suggest that most broad-lined SN Ic associated with low-luminosity GRBs in turn arise from a relatively small range of ZAMS progenitor masses, perhaps between 30 and 50 $M_\odot$. The detection of a similar SN in a highly luminous GRB extends this across a broader range of energy.

4.2. Host Galaxy

Our *HST* observations clearly resolve the afterglow from the host galaxy, showing the GRB to lie at a spatial offset of 0.″83

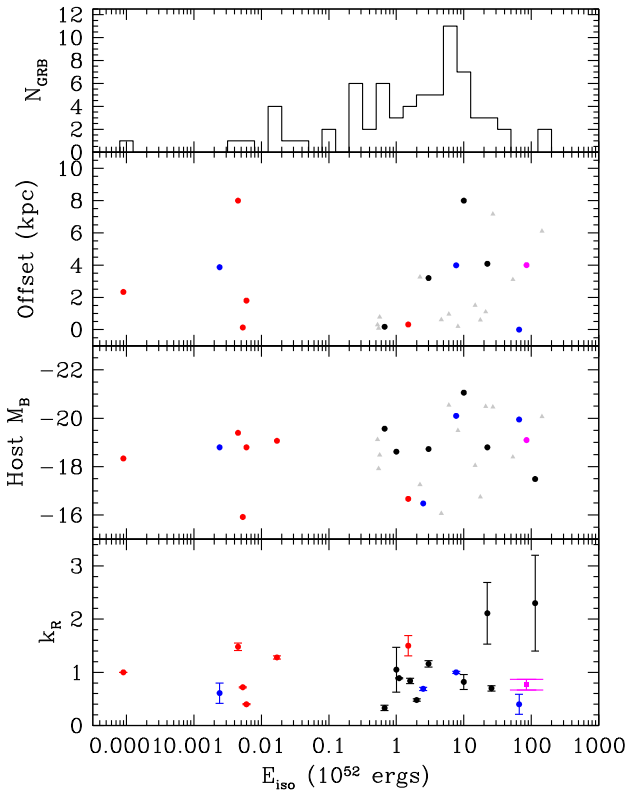

Figure 3. Top: a histogram of $E_{\rm iso}$ for *Swift* GRBs (from Kocevski & Butler 2008), amended with the $E_{\rm iso}$ values for GRB/SN pairs when not from *Swift*. Bottom: the *R*-band luminosities of candidate GRB/SN (scaled to SN 1998bw, which has $k_R = 1$), against the isotropic luminosities of the GRBs. Points in red are those with strong spectroscopic evidence for associated supernovae (category A in Hjorth & Bloom 2011), blue points indicate cases where spectral features were seen at lower signal-to-noise (category B in Hjorth & Bloom 2011), and black points are those with weaker evidence for associated SNe. The two errors bars marked in the case of SN 2013cq represent the error associated with a simple afterglow subtraction and the extrema of possibilities (see the text for details). The middle two panels show the offset from the GRB host center and the GRB host *B*-band absolute magnitude as a function of isotropic energy release. The color coding is the same as for the lower plot, while grey triangles indicate values from the literature for GRBs without claimed SNe associations (data from Bloom et al. 2002; Frail et al. 2001). These data show that the properties of GRB–SNe and host galaxies are largely unaffected by the energies of the burst, and hence that progenitors in similar environments and with similar initial masses can likely create the entire GRB luminosity function.

(A color version of this figure is available in the online journal.)

(4.0 kpc at $z = 0.34$) from the center of its host. This is a relatively large offset for a GRB from its host galaxy (>75% of those in Bloom et al. 2002) though by no means exceptional (see Figure 3). In the F606W observations, the galaxy exhibits a bar-like structure with a face-on disk visible beyond this, a weak spiral structure is also apparent, making the host one of few to be classified as a spiral (Svensson et al. 2010). The F336W imaging shows weak star formation close to the center of the galaxy, but the most striking feature is a strong star-forming region at a similar radial offset to the GRB, but offset from the GRB position by 0.″3 (1.5 kpc). This region is the strongest region of star formation in the host galaxy. While the magnitude of star formation underlying the GRB position remains uncertain because of contamination with the late-time afterglow, the offset region is at least a factor of ∼2 brighter. It also shows readily detectable O III emission in the late-time grism spectrum. The weak spiral arm in the direction of the GRB also appears distorted, and so it may be that star formation has been triggered via a tidal interaction. In the larger field around GRB 130427A, we note several galaxies of similar magnitude (see Figure 1). In our grism spectroscopy, these galaxies do not exhibit strong spectral lines, but they may well imply that the host of GRB 130427A lies within an association.

The magnitude of the galaxy in a large aperture at late times after the afterglow/SNe has significantly faded is F336W(AB) = 22.84 ± 0.07 at a rest-frame wavelength of approximately 2500 Å. This corresponds to a UV star-formation rate of $\sim 1.1 \pm 0.1\ M_\odot\ {\rm yr}^{-1}$ (error statistical only), broadly in agreement with that inferred from the SDSS observed spectral energy distribution of the galaxy of $2^{+5}_{-1}\ M_\odot\ {\rm yr}^{-1}$ (Xu et al. 2013) and suggesting a relatively (but not extremely) low specific star formation rate by the standards of GRB hosts (Svensson et al. 2010). The compact star-forming region close to the GRB contains ∼10% of this star formation, making a highly luminous star forming region comparable to that seen in the host of GRB 980425/SN 1998bw (Hammer et al. 2006; Christensen et al. 2008) or in a handful of other local galaxies (Beck et al. 1996). At late times, UV emission is visible close to the GRB position, indicating that lower level star formation is likely arising proximate to the GRB. This may still contain some afterglow light, but this region is at least a factor >1.5 fainter than the brightest star-forming region in the host.

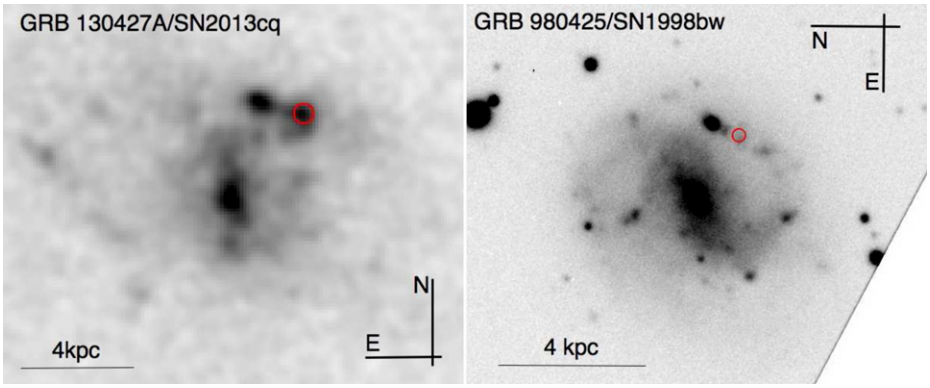

Figure 4. Host galaxies of GRB 130427A (left) and GRB 980425 (right). The left hand image is taken from our *HST* observations in F606W (2014 May), while the right-hand image is an archival image of the host obtained with VLT/FORS2 in 2004. The position of the GRB/SNe is marked with a red circle in each case (note that the GRB 130427A image may contain afterglow contribution at the GRB/SN position). The resemblance between the two host galaxies is striking, especially given the rarity of spiral hosts among GRB host galaxies. Interestingly, unlike most bursts, these do not lie on the brightest regions of the hosts, but in spiral arms where the metallicity may be lower (see Fruchter et al. 2006). In both GRB 130427A and GRB 980425 the GRB/SNe occurred in a relatively faint region within the spiral arm and not in the strongest star-forming complex.

(A color version of this figure is available in the online journal.)

Some previously extremely energetic bursts (e.g., GRB 080319B; Tanvir et al. 2010) have shown extremely faint and small host galaxies, while the hosts of GRBs 980425, 030329, and 060218 are also sub-luminous and LMC-like. However, as show in Figure 3 the overall population of GRB–SN host luminosities shows no discernible correlation with the energy of the GRB (see also Levesque et al. 2010), and the host of GRB 130427A is in keeping with these expectations. It is intriguing to note that the GRB host galaxy with the closest properties to that of GRB 130427A/SN 2013cq is in fact the host of SN 1998bw. It is also a rare example of a spiral galaxy, in which the GRB occurs at a moderately large offset from the nucleus and from the strongest region of star formation within the host galaxy. This is shown graphically in Figure 4. Given the similarities in SN and environment, GRB 130427A would seem like a close analog of GRB 980425A if it were not for the factor of 10^6 difference in their γ-ray energy releases.

5. CONCLUSIONS

We have presented *HST* imaging and spectroscopic observations of the extremely bright GRB 130427A, which show that it was associated with a luminous broad line SN Ic (SN 2013cq). The red spectra offer good agreement with those of SN 1998bw, while the bluer spectra appear well-matched in position if not shape with SN 2010bh. The host galaxy appears to be a disk galaxy of moderate luminosity and star-formation rate, whose overall characteristics are consistent with those of the GRB host population at large. The similar properties of the SNe and hosts over six orders of magnitude in GRB isotropic equivalent energy would appear to suggest that the energy of the GRB is not a strong function of environment or the mass of the progenitor star, and that stars of similar mass and composition are responsible for the entire luminosity function of GRBs. More complex effects within the star (e.g., rotation) or geometric effects are therefore needed to explain much of the diversity in the GRB luminosity function.

We thank Matt Mountain and the STScI staff for rapidly scheduling our observations. A.J.L. thanks the Leverhulme Trust. A.J.L., N.R.T., and K.W. are supported by STFC. The Dark Cosmology Centre is funded by the DNRF. Based on observations made with the NASA/ESA *Hubble Space Telescope*, obtained at the Space Telescope Science Institute, which is operated by the Association of Universities for Research in Astronomy, Inc., under NASA contract NAS 5-26555. These observations are associated with program Nos. 13230, 13110, and 13117.

REFERENCES

Anderson, J. 2014, Instrument Science Report, WFC3 2014-02 (Baltimore, MD: STScI)
Anderson, J., & ACS Team 2012, BAAS, 219, 241.04
Beck, S. C., Turner, J. L., Ho, P. T. P., Lacy, J. H., & Kelly, D. M. 1996, ApJ, 457, 610
Bloom, J. S., Kulkarni, S. R., & Djorgovski, S. G. 2002, AJ, 123, 1111
Bufano, F., Pian, E., Sollerman, J., et al. 2012, ApJ, 753, 67
Campana, S., Mangano, V., Blustin, A. J., et al. 2006, Natur, 442, 1008
Cano, Z. 2013, arXiv e-prints
Cano, Z., Bersier, D., Guidorzi, C., et al. 2011, ApJ, 740, 41
Christensen, L., Vreeswijk, P. M., Sollerman, J., et al. 2008, A&A, 490, 45
de Ugarte Postigo, A., Xu, D., Leloudas, G., et al. 2013, CBET, 3529, 1
Fitzpatrick, E. L. 1999, PASP, 111, 63
Frail, D. A., Kulkarni, S. R., Sari, R., et al. 2001, ApJL, 562, L55
Fruchter, A. S., Levan, A. J., Strolger, L., et al. 2006, Natur, 441, 463
Galama, T. J., Vreeswijk, P. M., van Paradijs, J., et al. 1998, Natur, 395, 670
Hammer, F., Flores, H., Schaerer, D., et al. 2006, A&A, 454, 103
Hjorth, J., & Bloom, J. S. 2011, arXiv:1104.2274
Hjorth, J., Sollerman, J., Møller, P., et al. 2003, Natur, 423, 847
Iwamoto, K., Mazzali, P. A., Nomoto, K., et al. 1998, Natur, 395, 672
Kaneko, Y., Ramirez-Ruiz, E., Granot, J., et al. 2007, ApJ, 654, 385
Kocevski, D., & Butler, N. 2008, ApJ, 680, 531
Levan, A., Patel, S., Kouveliotou, C., et al. 2005, ApJ, 622, 977
Levan, A. J., Cenko, S. B., Perley, D. A., & Tanvir, N. R. 2013, GCN, 14455, 1
Levan, A. J., Tanvir, N. R., Starling, R. L. C., et al. 2014, ApJ, 781, 13
Levesque, E. M., Soderberg, A. M., Kewley, L. J., & Berger, E. 2010, ApJ, 725, 1337
Maselli, A., Beardmore, A. P., Lien, A. Y., et al. 2013, GCN, 14448, 1
Maselli, A., Melandri, A., Nava, L., et al. 2014, Sci, 343, 48
Mazzali, P. A., Deng, J., Tominaga, N., et al. 2003, ApJL, 599, L95
Melandri, A., Pian, E., D'Elia, V., et al. 2014, A&A, 567, 29
Mazzali, P. A., Walker, E. S., Pian, E., et al. 2013, MNRAS, 432, 2463
Nakar, E., & Sari, R. 2012, ApJ, 747, 88
Olivares E., F., Greiner, J., Schady, P., et al. 2012, A&A, 539, A76
Patat, F., Cappellaro, E., Danziger, J., et al. 2001, ApJ, 555, 900
Perley, D. A., Cenko, S., Other, A., et al. 2014, ApJ, 781, 37
Pian, E., Mazzali, P. A., Masetti, N., et al. 2006, Natur, 442, 1011
Sirianni, M., Jee, M. J., Benítez, N., et al. 2005, PASP, 117, 1049
Soderberg, A. M., Kulkarni, S. R., Berger, E., et al. 2004, Natur, 430, 648
Sparre, M., & Starling, R. L. C. 2012, MNRAS, 427, 2965
Stanek, K. Z., Matheson, T., Garnavich, P. M., et al. 2003, ApJL, 591, L17
Starling, R. L. C., Levan, A. J., Wiersema, K., et al. 2012, GCN, 13911, 1
Starling, R. L. C., Wiersema, K., Levan, A. J., et al. 2011, MNRAS, 411, 2792
Svensson, K. M., Levan, A. J., Tanvir, N. R., Fruchter, A. S., & Strolger, L.-G. 2010, MNRAS, 405, 57
Šimon, V., Pizzichini, G., & Hudec, R. 2010, A&A, 523, A56
Tanvir, N. R., Rol, E., Levan, A. J., et al. 2010, ApJ, 725, 625
von Kienlin, A. 2013, GCN, 14473, 1
Wren, J., Vestrand, W. T., Wozniak, P., & Davis, H. 2013, GCN, 14476, 1
Xu, D., de Ugarte Postigo, A., Leloudas, G., et al. 2013, ApJ, 776, 98
Zhu, S., Racusin, J., Chiang, J., & Vianello, G. 2013, GCN, 14508, 1